BMC Medical Genomics

RESEARCH

Open Access

Comprehensive pan-cancer analysis of HSPG2 as a marker for prognosis

Fangjun Chen[1†], Xing Gu[2†] and Guangliang Qiang[3*]

Abstract

Background In recent years, several studies have shown that HSPG2 is associated with the prognosis of specific cancers. The aim of this study was to investigate the prognostic value of HSPG2 in pan-cancer and to analyze its possible mechanisms.

Methods We used The Cancer Genome Atlas (TCGA) and Genotype-Tissue Expression (GTEx) to explore the expression of HSPG2 in 33 tumors and corresponding controls. Univariate Cox regression and Kaplan–Meier survival analysis were applied to detect the effects of HSPG2 on overall survival (OS), disease-specific survival (DSS), and progression-free interval (PFI) in patients with these tumors, and to analyze the relationship between HSPG2 and clinical characteristics. And we further analyzed the relationship between HSPG2 and immune infiltration, DNA methylation and single cell function. And GO and KEGG enrichment analyses were performed using HSPG2 co-expressed genes. Finally, we explored the diagnostic efficacy of HSPG2 for diseases of interest and validated it using qPCR experiment.

Results HSPG2 was lowly expressed in 17 cancers and highly expressed in 11 cancers, and was correlated with patient's clinical characteristics in many cancers. Multivariate regression analysis showed that HSPG2 was an independent prognostic factor for DSS, OS, and PFI in bladder urothelial carcinoma (BLCA) and Mesothelioma (MESO). HSPG2 was correlated with DNA methylation, single-cell function, and immune infiltration in a variety of cancers. HSPG2 exhibited a good diagnostic efficacy for BLCA and MESO. qPCR and western blot results showed that HSPG2 expression was increased in mesothelioma compared to normal controls.

Conclusion These findings suggest that HSPG2 could be considered as a potential diagnostic and prognostic marker for BLCA and MESO.

Keywords Pan cancer, HSPG2, Prognosis, Diagnosis, BLCA, MESO

Introduction

Cancer is the leading cause of death and a major obstacle to increasing life expectancy worldwide [1]. And cancer incidence has increased among adolescents and young adults (AYAs), but mortality has decreased significantly between 1990 and 2019 [2]. The resulting healthcare burden looms large. It is estimated that in 2024, 611,720 people will die of cancer in the United States, equating to about 1,680 deaths per day, and cancer patients are increasingly shifting from the elderly to the middle-aged [3]. This is also similar in China, where cancer incidence has increased for all cancers among young people aged

†Fangjun Chen and Xing Gu contributed equally to this work.

*Correspondence:
Guangliang Qiang
pkudd@bjmu.edu.cn
[1] Department of Thoracic Surgery, China-Japan Friendship Institute of Clinical Medicine, No.2 Yinghua East Street, Chaoyang District, Beijing 100029, China
[2] College of Foreign Languages, Chongqing Medical University, No.1 Yixueyuan Road, Yuzhong District, Chongqing 400016, China
[3] Department of Thoracic Surgery, Peking University Third Hospital, No.49 Huayuan North Road, Haidian District, Beijing 100191, China

20–49, with the highest average annual percent change (AAPC) (1.46%) among adults aged 20–24 [4].

Perlecan (also known as heparan sulfate proteoglycan 2 (HSPG2)) is a ubiquitous HS proteoglycan synthesized by most cells, found in most pericellular and extracellular matrices, and considered to be an essential component of the basement membrane [5, 6]. The protein core of human perlecan is 460 kDa and consists of five distinct structural domains with glycosaminoglycan attachment sites located in the N-terminal and C-terminal domains. Perlecan exerts its tissue-specific activity through its glycosaminoglycan chains and the structure of these chains depends on the environment and the cellular origin [7].

Previous studies have suggested that HSPG2 may be associated with a variety of tumors. It may be associated with cell behavior, microenvironment, and aggressiveness in prostate cancer [8–10], prognosis of patients with AML [11], prognosis of patients with chemotherapy-resistant and triple-negative breast cancer [12, 13], immune checkpoint inhibitor outcomes in melanoma and non-small-cell lung cancer [14], prognosis of patients with oligoastrocytoma, oligodendroglioma, and glioblastoma [15, 16], metastasis and drug-resistance in pancreatic cancer cells [17], and melanoma aggressiveness [18], colorectal cancer [19], aggressiveness and prognosis of lung cancer [20, 21], prognosis of bladder cancer patients [22], and prognosis of gastric cancer patients [23].

Although the studies mentioned above have shown the role of HSPG2 in some cancers, the literature for some cancer types is too old without similar studies in recent years, and some studies included a small sample size of subjects. In this case, it is particularly important to analyze the role and value of HSPG2 in pan-cancer using a larger sample size. Therefore, this study intends to conduct a pan-cancer study of HSPG2 to explore the value of HSPG2 in pan-cancer and to analyze its possible mechanisms.

Methods

This study was carried out in accordance with the Declaration of Helsinki.

Gene expression and subcellular localization analysis of HSPG2 in pan-cancer

The TIMER database (http://cistrome.dfci.harvard.edu/TIMER/, accessed on March 6, 2024) is an analytical network for tumor immune cell infiltration, and it can analyze differential gene expression between tumor tissues and normal tissues [24].

In addition, since some of the tumors in TCGA lacked normal tissues, we also utilized the Xiantao Academic (https://www.xiantaozi.com/) online analysis tools (including RNA-seq data for 33 cancers from The Cancer Genome Atlas (TCGA) database and the Genotypic Tissue Expression (GTEx) database) to analyze the expression of HSPG2 in tumor and normal tissues. Significant differences were analyzed by Wilcoxon tests. In addition, we determined the subcellular localization of HSPG2 by indirect immunofluorescence microscopy (https://www.proteinatlas.org/search/, accessed on March 6, 2024) [25]. The abbreviations of the 33 tumors are shown in Table 1.

Table 1 Pan-cancers and the corresponding abbreviations

Cancer Type	Abbreviation
Adrenocortical carcinoma	ACC
Bladder Urothelial Carcinoma	BLCA
Breast invasive carcinoma	BRCA
Cervical squamous cell carcinoma and endocervical adenocarcinoma	CESC
Cholangiocarcinoma	CHOL
Colon adenocarcinoma	COAD
Lymphoid Neoplasm Diffuse Large B-cell Lymphoma	DLBC
Esophageal carcinoma	ESCA
Glioblastoma multiforme	GBM
Head and Neck squamous cell carcinoma	HNSC
Kidney Chromophobe	KICH
Kidney renal clear cell carcinoma	KIRC
Kidney renal papillary cell carcinoma	KIRP
Acute Myeloid Leukemia	LAML
Brain Lower Grade Glioma	LGG
Liver hepatocellular carcinoma	LIHC
Lung adenocarcinoma	LUAD
Lung squamous cell carcinoma	LUSC
Mesothelioma	MESO
Ovarian serous cystadenocarcinoma	OV
Pancreatic adenocarcinoma	PAAD
Pheochromocytoma and Paraganglioma	PCPG
Prostate adenocarcinoma	PRAD
Rectum adenocarcinoma	READ
Sarcoma	SARC
Skin Cutaneous Melanoma	SKCM
Stomach adenocarcinoma	STAD
Testicular Germ Cell Tumors	TGCT
Thyroid carcinoma	THCA
Thymoma	THYM
Uterine Corpus Endometrial Carcinoma	UCEC
Uterine Carcinosarcoma	UCS
Uveal Melanoma	UVM

Relationship between HSPG2 and clinicopathologic features

The Wilcoxon test was used to explore the correlation between HSPG2 expression and clinicopathologic features, including T stage, N stage, M stage, stage, age, and gender. Correlation analyses were completed using the Xiantao Academic (https://www.xiantaozi.com/) online analysis tool.

Prognostic analysis of HSPG2

We chose overall survival (OS), disease-specific survival (DSS) and progression-free interval (PFI) to analyze the correlation between HSPG2 expression and the prognosis of 33 cancers. Patients were categorized into high and low HSPG2 groups based on the median HSPG2 expression value with 50% cut-off high and 50% cut-off low [26]. Kaplan–Meier survival analysis and Cox regression were performed to explore the correlation between HSPG2 and survival prognosis. Correlation analyses were completed using the Xiantao Academic (https://www.xiantaozi.com/) online analysis tool.

Gene mutation analysis of HSPG2

cBioPortal (https://www.cbioportal.org/, accessed on March 6, 2024) is a web platform for analyzing tumor genomic characteristics in the HSPG2 gene. We used this database to analyze the frequency of pan-cancer mutations in HSPG2 [27]. Mutational alterations included mutation, amplification and deep deletion.

Relationship between HSPG2 and immunity

The TIMER database (http://cistrome.dfci.harvard.edu/TIMER/, accessed on March 6, 2024) was used to analyze the relationship between HSPG2 and tumor immune cell infiltration [28]. It can generate a functional heatmap table, enabling the user to easily identify significant associations in multiple cancer types simultaneously, such as cancer associated fibroblasts, endothelial cell and hematopoietic stem cell.

Correlation study of HSPG2 with TMB and MSI

TMB is defined as the total number of base mutations per million cells in a tumor. It is widely believed that TMB can stimulate the production of tumor-specific and high-immunogen antibodies and is a novel target for predicting the efficacy of tumor immunotherapy [29]. MSI is caused by DNA MMR abnormalities, which lead to gene duplication disorders and tumor development, affecting the prognosis of tumors [30–32]. Spearman's correlation was used to analyze the correlation of HSPG2 with TMB and MSI.

DNA methylation analysis of HSPG2

DNA methylation is a common form of epigenetic modification. Abnormal DNA methylation may exist in tumor cells [33]. We searched the UALCAN database (http://ualcan.path.uab.edu/, accessed March on 7, 2024) to explore the level of HSPG2 promoter DNA methylation in certain cancers to identify differences between tumors and normal tissues. Shiny Methylation Analysis Resource Tool (SMART, http://www.bioinfo-zs.com/smartapp/, accessed on March 7, 2024) was used to discuss the distribution of methylated probes in chromosomes [34].

Single-cell functional analysis of HSPG2

The Cancer single-cell state atlas (CancerSEA, http://biocc.hrbmu.edu.cn/CancerSEA/, accessed on March 7, 2024) is an analytical tool used to study cancer cell function(such as metastasis, stemness, invasion, and proliferation) at the single-cell level and contains 14 tumor-associated cellular functions of 900 cancer cells from 25 cancers [35].

Co-expressed genes and enrichment analysis of HSPG2

GeneMANIA (http://genemania.org/, accessed on March 7, 2024) is an online tool for exploring gene interactions and functions and identifying co-expressed genes [36]. Nineteen genes co-expressed with HSPG2 were obtained through GeneMANIA. Gene Ontology (GO) and Kyoto Encyclopedia of Genes and Genomes (KEGG) enrichment were conducted using the Bioinformatics online platform (https://www.bioinformatics.com.cn/).

Diagnostic efficacy of HSPG2 for BLCA and MESO and qPCR results

We searched the GEO and TCGA databases and further explored the expression difference and diagnostic efficacy of HSPG2 for BLCA and MESO using the datasets GSE13507 (including 165 cases of primary tumors, 9 cases of normal bladder mucosa, and 58 cases of paracarcinoma mucosal tissues) and GSE51024 (including 55 tumor samples and 41 paired samples), respectively.

To further investigate the positive results we were interested in and to verify the accuracy of the conclusions, we performed qPCR experiments on the tumor cell lines and the corresponding normal cell lines to test whether there was a difference in the expression of HSPG2. Correlation analysis was conducted using the normal uroepithelial cell line Ku-1919 (icell-h473, iCell Bioscience Inc., China) and the bladder cancer cell line SV-HUC-1 (CL-0222) provided by Pricella Life Science&Technology Co.,Ltd, mesothelioma cell line NCI-H2452 [H2452] (CL-0398)

and normal mesothelial cell line MET-5A (CL-0666). The medium information for each cell line was as follows: Ku-1919 (RPMI-1640 + 10% FBS + 1% P/S), SV-HUC-1 (Ham's F-12 K + 10% FBS + 1% P/S), H2452 (RPMI-1640 + 10% FBS + 1% P/S), MET-5A (M199 with 10% FBS complete medium). SteadyPure Quick RNA Extraction Kit, Evo M-MLV RT Mix Kit with gDNA Clean for qPCR Ver.2, SYBR Green Premix Pro TaqHS qPCR Kit III (Low Rox Plus) and primers for the target genes were purchased from ACCURATE BIOTECHNOLOGY (HUNAN) CO., LTD. The expression levels of the target genes were determined using the QuantStudio™ 5 System with human β-actin as a control. The following primers were used: human β-actin: 5'-TGGCACCCAGCACAA TGAA-3'(primer F) and 5'-CTAAGTCATAGTCCGCCT AGAAGCA-3'(primer R); human HSPG2: 5'-GACGGC TCTTTCCACCTGAG-3' (primer F), 5'-CGACTGACA CCCATGCAGAA-3' (primer R). Subsequently, delta-delta Ct method was used for data statistics.

Total protein was obtained from each sample using RIPA lysis buffer (Beyotime, China) supplemented with 1 μM phenylmethanesulfonyl fluoride (PMSF, Beyotime, China). Then, twenty microgram of protein was separated by sodium dodecyl sulfate–polyacrylamide gel electrophoresis (SDS-PAGE, YAMEI, China) and transferred onto polyvinylidene fluoride membranes (PVDF, Millipore, USA). Subsequently, membranes were blocked with 5% non-fat milk for 2 h at room temperature, followed by incubation with primary antibodies at 4 °C overnight. The primary antibodies used in this study were anti-HSPG2 (Abcam, UK, ab255829) used at 1:1000 and anti-vinculin (ABclonal, China, A1758) used at 1:1000 diluted in primary antibody dilution buffer (Beyotime, China, P0256). The membranes were washed and exposed to corresponding horseradish peroxidase (HRP)-conjugated goat anti-mouse (1:1000, Beyotime, China, A0216) or goat anti-rabbit (1:1000, Beyotime, China, A0208) secondary antibodies diluted in TBST buffer for 1 h at room temperature. Finally, the protein bands were visualized with an enhanced chemiluminescence (ECL) kit (Beyotime, China,P0018FM), and the band intensity was analyzed using OI-capture software (BIO-OI, China, OI900 MF).

Statistical analysis

Wilcoxon test was applied to study HSPG2 expression and its correlation with clinical features based on TCGA and GTEx databases. Spearman correlation analysis estimated the correlation of HSPG2 with TMB and MSI. Follow-up correlation analyses were performed using a variety of online analysis websites; $p < 0.05$ indicates statistical significance. The receiver operating characteristic (ROC) curve was used to investigate the diagnostic efficacy of HSPG2 for BLCA and MESO.

Results

Analysis of gene expression and subcellular localization of HSPG2 in pan-cancer

The TIMER database was used to analyze the expression of HSPG2 in pan-cancer and normal tissues. The results showed that HSPG2 expression was up-regulated in 7 cancers, including CHOL, GBM, HNSC, KIRC, LIHC, STAD and THCA, and it was down-regulated in 6 cancers, including BLCA, CESC, KICH, KIRP, PRAD and UCEC, as compared with normal tissues (Fig. 1a). Since some tumors in TIMER had no corresponding normal tissues, we combined TCGA and GTEx to study HSPG2 expression in 33 tumors and found that HSPG2 expression was up-regulated in 11 tumors compared to corresponding normal tissues, including CHOL, DLBC, GBM, HNSC, KIRC, LGG, LIHC, OV, PAAD, STAD and THYM, and it was down-regulated in 17 cancers, including ACC, BLCA, BRCA, CESC, COAD, ESCA, KICH, KIRP, LAML, LUAD, LUSC, PRAD, READ, SKCM, THCA, UCEC, and UCS (Fig. 1b). The results were generally consistent except for THCA.

The subcellular localization of HSPG2 was obtained from online data by immunofluorescence localization of nuclei, microtubules and endoplasmic reticulum in A-431, U-2OS and U-251 MG cells. The results showed that HSPG2 was found in Nucleoplasm, Plasma membrane and Cytosol in all 3 cells (Fig. 1C). These results further indicate the universality of HSPG2 and the possibility of targeting HSPG2.

Relationship between HSPG2 and clinicopathological features

Subsequently, we explored the association between HSPG2 and clinicopathologic features. The details are shown in Fig. 2. The results showed that HSPG2 expression was higher in the higher T stage of urinary BLCA and KIRP, and in the lower T stage of THCA and KIRC (Fig. 2a). HSPG2 expression was lower in higher N stage of LUSC, and higher in higher N stage of KIRC (Fig. 2b). HSPG2 expression was lower than M0 in patients with M1-stage KIRC (Fig. 2c). HSPG2 expression was higher in the higher stages of BLCA and KIRP, and in the lower stages of THCA and KIRC (Fig. 2d). HSPG2 expression was higher in older patients with LUSC and THCA, and lower in older patients with TGCT, COAD and KIRP (Fig. 2e). HSPG2 expression was higher in male patients with SKCM and higher in female patients with LIHC and KIRP (Fig. 2f).

Prognostic value of HSPG2

We chose OS, DSS and PFI to study the prognosis of HSPG2 in pan-cancer. Univariate analysis showed that

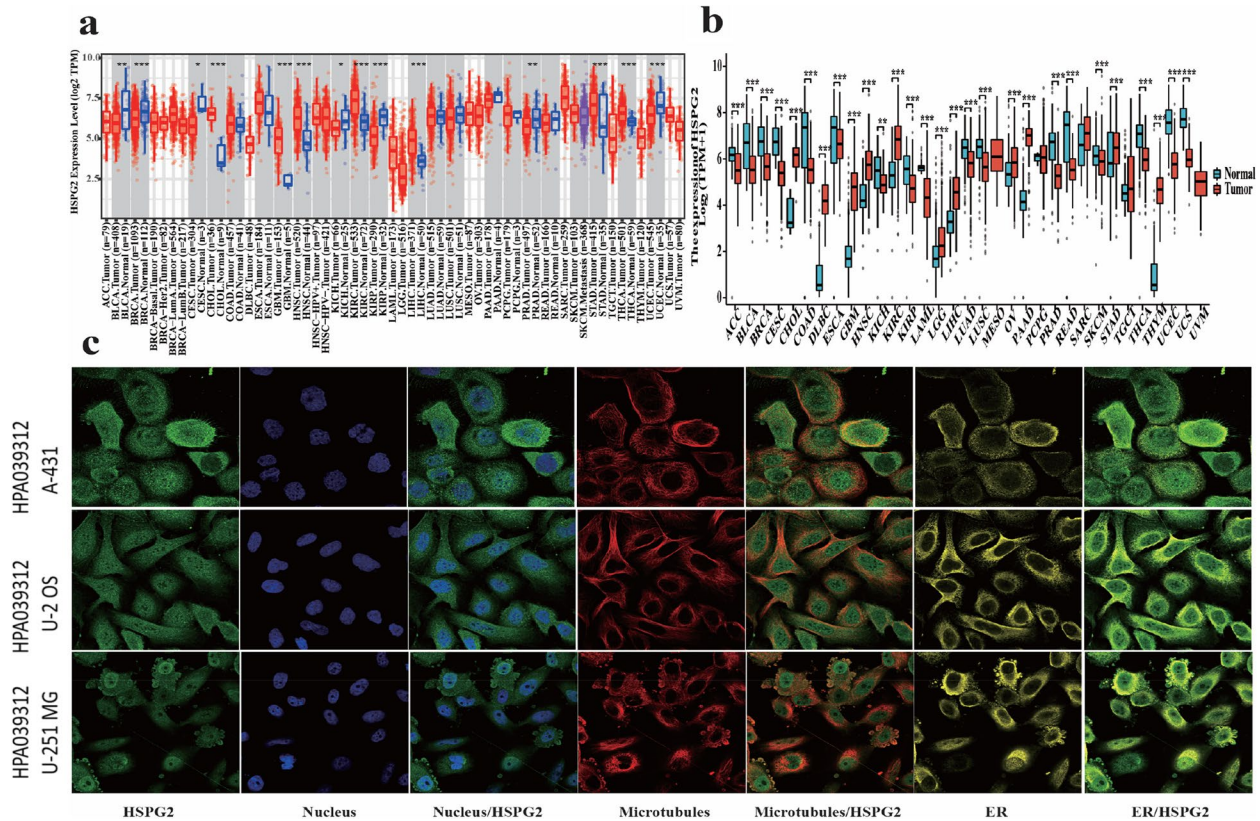

Fig. 1 Expression and subcellular localization of HSPG2. **a** Expression of HSPG2 in pan-cancer and control in TIMER database; **b** Expression of HSPG2 in pan-cancer and control in Xiantao Academic Online database; **c** Subcellular localization of HSPG2

high expression of HSPG2 had better OS, DSS, and PFI in KIRC, but shorter OS, DSS, and PFI in BLCA, LGG, and MESO. Moreover, high expression of HSPG2 had shorter OS and DSS in OV, and shorter PFI in ACC and COAD. The results are shown in Fig. 3a-c. Multivariate analysis showed that high expression of HSPG2 had shorter OS, DSS and PFI in BLCA and MESO, but low expression of HSPG2 had shorter OS in KIRC. The results are shown in Tables 2, 3, and 4. These findings suggested that HSPG2 may be an independent prognostic marker for BLCA and MESO.

Gene mutation analysis of HSPG2

We discussed HSPG2 genetic alterations in pan-cancer using the cBioPortal database. The highest frequency of genetic variation in HSPG2 was found in SKCM, mainly in the form of mutation. The second and third highest frequencies of HSPG2 occurred in UCEC and STAD, also mainly in the form of mutation (Fig. 4). These results indicate that HSPG2 is mutated in a variety of cancers and in a variety of ways.

Relationship between HSPG2 and immunity

The results showed that the expression of HSPG2 was positively correlated with cancer-associated fibroblasts, endothelial cells, and hematopoietic stem cells of various tumors(including BLCA and MESO). Details are shown in Fig. 5a-c. These results suggest that the association between HSPG2 and cancer may be caused by influencing the degree of infiltration of various immune cells.

Relationship between HSPG2 and TMB, MSIs

We also performed a correlation analysis of HSPG2 expression with TMB and MSI, which were significantly correlated with immune checkpoint inhibitors (ICIs) sensitivity. The results showed that HSPG2 was positively correlated with TMB in LGG and THYM, whereas it was negatively correlated with TMB in BLCA, BRCA, LIHX, LUAD and STAD (Fig. 6a). Furthermore, HSPG2 was positively correlated with MSI in CESC, COAD, KIRC, LUSC, TGCT, and UVM, while it was negatively correlated with MSI in BRCA, DLBC, STAD, and THCA (Fig. 6b). The results suggest that patients with different

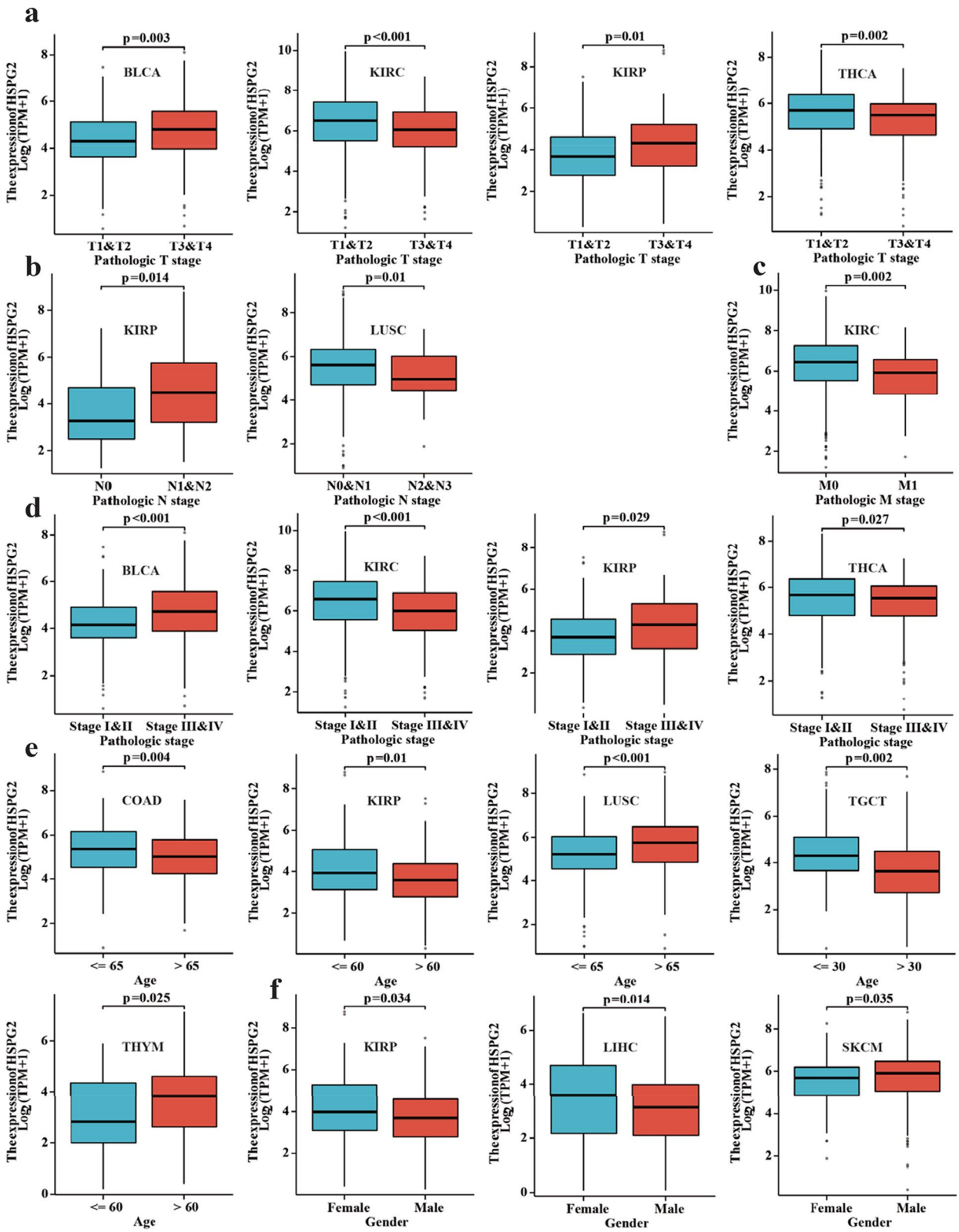

Fig. 2 Relationship between HSPG2 and clinical features. **a** Relationship between HSPG2 and T stage; **b** relationship between HSPG2 and N stage; **c** relationship between HSPG2 and M stage; **d** relationship between HSPG2 and staging; **e** relationship between HSPG2 and age; **f** relationship between HSPG2 and gender

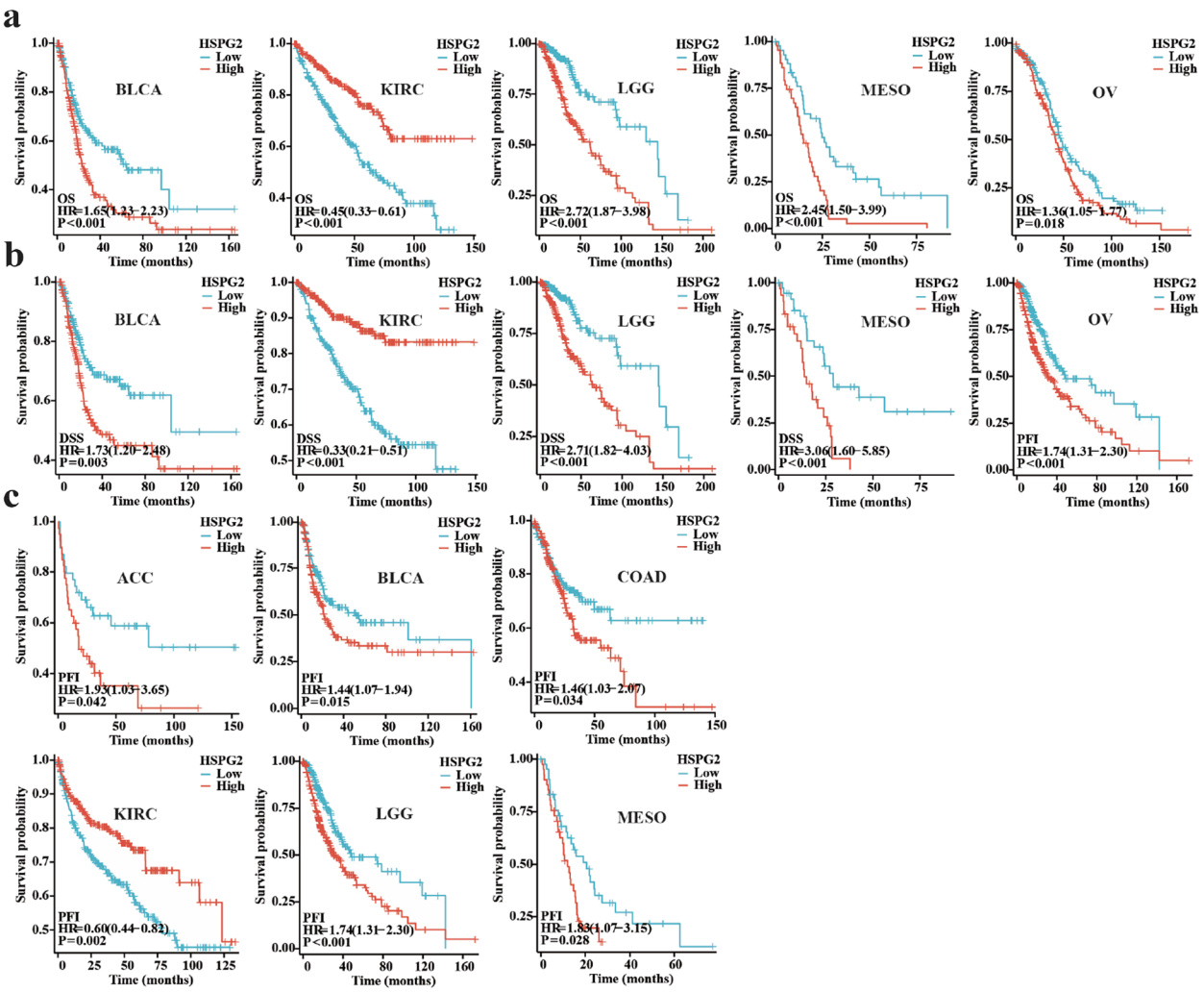

Fig. 3 Relationship between HSPG2 and prognosis. **a** Relationship between HSPG2 and OS; **b** relationship between HSPG2 and DSS; **c** relationship between HSPG2 and PFI

HSPG2 expression need personalized drug treatment strategies.

DNA methylation analysis of HSPG2

We examined the DNA methylation level of HSPG2 in various tumors using the UALCAN database, and the results showed that the methylation level of HSPG2 was higher than that of normal tissues in BLCA, BRCA, CESC, COAD, ESCA, HNSC, KIRC, KIRP, LUAD, LUSC, PRAD, READ, and THCA, which might be an explanation for the low expression of HSPG2 in these tumors. The methylation level of HSPG2 in LIHC, PCPG and TGCT was lower than that in normal tissues (Fig. 7a). In addition, HSPG2 had 58 methylation probes, such as cg00309945, cg21876283, cg10538929, cg06782041, cg24254377, cg16384073, cg06909773, cg13430401, cg11821759, cg21616627, cg24447680, cg02583234, cg11419235, cg02459271, cg11818031, cg25940827, cg17420036, cg13242624, cg26433593, cg04117379, cg14282182, cg11839036, cg18941458, cg12257830, cg18274749, cg22817258, cg18861547, cg10820203, cg02956660, cg13940218, cg02117102, cg27304144, cg18240311, cg20103919, cg04852275, cg00543840, cg03977084, cg07172756, cg18221576, cg24109161, cg13063658, cg04573706, cg12409547, cg25138553, cg00359395, cg24332002, cg13215285, cg06161657, cg07142131, cg04297819, cg13357518, cg02729506, cg15009352, cg15011041, cg24075852, cg14380609, cg12274479, cg01794853 (Fig. 7b).

Single-cell functional analysis of HSPG2

To further study the potential role of HSPG2 in tumors, we investigated the function of HSPG2 at the single-cell level using CancerSEA (Fig. 8a). The results showed that

Table 2 Multivariate COX analysis of HSPG2 and BLCA prognosis

	OS					DSS					PFI				
	Univariate analysis			Multivariate analysis		Univariate analysis			Multivariate analysis		Univariate analysis			Multivariate analysis	
Characteristics	Total(N)	HR(95% CI)	*P* value	HR(95% CI)	*P* value	Total(N)	HR(95% CI)	*P* value	HR(95% CI)	*P* value	Total(N)	HR(95% CI)	*P* value	HR(95% CI)	*P* value
Pathologic T stage	377					364					378				
T1	5	Reference		Reference		5	Reference		Reference		5	Reference		Reference	
T2	118	5,916,824.2028 (0.000—Inf)	0.993	2,532,492.7659 (0.000—Inf)	0.997	118	5,903,041.0662 (0.000—Inf)	0.994	2,105,780.4302 (0.000—Inf)	0.998	118	0.397 (0.140—1.122)	0.081	28,350,182.8668 (0.000—Inf)	0.999
T3	195	11,004,504.7767 (0.000—Inf)	0.992	3,302,267.1043 (0.000—Inf)	0.997	184	11,068,411.8048 (0.000—Inf)	0.994	2,348,989.5659 (0.000—Inf)	0.998	196	0.774 (0.284—2.110)	0.617	54,521,478.9483 (0.000—Inf)	0.999
T4	59	16,681,977.3123 (0.000—Inf)	0.992	2,797,375.5060 (0.000—Inf)	0.997	57	17,223,959.9614 (0.000—Inf)	0.993	2,618,174.4008 (0.000—Inf)	0.998	59	1.344 (0.475—3.806)	0.577	33,987,351.8957 (0.000—Inf)	0.999
Pathologic N stage	367					355					368				
N0	238	Reference		Reference		232	Reference		Reference		238	Reference		Reference	
N1	46	1.844 (1.189—2.857)	0.006	1.128 (0.417—3.053)	0.813	45	2.754 (1.662—4.563)	< 0.001	1.324 (0.385—4.554)	0.656	46	2.377 (1.537—3.676)	< 0.001	0.745 (0.278—2.000)	0.560
N2	77	2.534 (1.781—3.606)	< 0.001	2.080 (0.815—5.313)	0.126	72	3.437 (2.229—5.299)	< 0.001	3.578 (1.160—11.034)	0.027	77	2.931 (2.031—4.232)	< 0.001	2.523 (0.968—6.579)	0.058
N3	6	2.410 (0.759—7.654)	0.136	5.035 (0.296—85.67)	0.264	6	4.133 (1.279—13.35)	0.018	37.956 (1.587—907.8)	0.025	7	7.438 (2.969—18.63)	< 0.001	52.294 (5.092—537.1)	< 0.001
Pathologic M stage	212					207					212				
M0	201	Reference		Reference		196	Reference		Reference		201	Reference		Reference	
M1	11	3.112 (1.491—6.493)	0.002	0.354 (0.070—1.781)	0.208	11	4.171 (1.874—9.282)	< 0.001	0.089 (0.011—0.707)	0.022	11	6.416 (3.099—13.286)	< 0.001	0.269 (0.047—1.547)	0.141
Histologic grade	408					394					409				
High grade	387	Reference				373	Reference				388	Reference		Reference	
Low grade	21	0.338 (0.084—1.365)	0.128			21	0.464 (0.114—1.884)	0.283			21	0.274 (0.068—1.107)	0.069	0.000 (0.000—Inf)	0.998
Primary therapy outcome	355					352					355				
PD	70	Reference		Reference		69	Reference		Reference		70	Reference		Reference	
SD	30	0.555 (0.325—0.949)	0.031	0.492 (0.139—1.739)	0.271	30	0.476 (0.267—0.848)	0.012	0.278 (0.064—1.207)	0.087	30	0.623 (0.384—1.012)	0.056	0.803 (0.288—2.241)	0.676

Table 2 (continued)

	OS					DSS					PFI				
	Univariate analysis			Multivariate analysis		Univariate analysis			Multivariate analysis		Univariate analysis			Multivariate analysis	
Characteristics	Total(N)	HR(95% CI)	*P* value	HR(95% CI)	*P* value	Total(N)	HR(95% CI)	*P* value	HR(95% CI)	*P* value	Total(N)	HR(95% CI)	*P* value	HR(95% CI)	*P* value
PR	22	0.697 (0.398—1.218)	0.205	0.916 (0.255—3.297)	0.893	21	0.740 (0.416—1.317)	0.306	0.649 (0.162—2.601)	0.542	22	0.542 (0.315—0.933)	0.027	0.708 (0.207—2.422)	0.582
CR	233	0.155 (0.105—0.228)	< 0.001	0.202 (0.074—0.547)	0.002	232	0.074 (0.045—0.120)	< 0.001	0.068 (0.020—0.235)	< 0.001	233	0.099 (0.068—0.145)	< 0.001	0.102 (0.040—0.260)	< 0.001
Gender	411					397					412				
Female	108	Reference				102	Reference				108	Reference			
Male	303	0.868 (0.629—1.198)	0.390			295	0.877 (0.593—1.296)	0.510			304	0.911 (0.655—1.266)	0.578		
Age	411					397					412				
< =70	231	Reference		Reference		224	Reference				232	Reference			
> 70	180	1.424 (1.064—1.906)	0.018	0.999 (0.469—2.125)	0.997	173	1.031 (0.721—1.474)	0.868			180	1.066 (0.791—1.435)	0.676		
BMI	361					351					362				
< =25	151	Reference				146	Reference				152	Reference			
> 25	210	1.000 (0.721—1.386)	0.998			205	1.069 (0.718—1.591)	0.743			210	1.073 (0.776—1.484)	0.669		
Subtype	406					392					407				
Non-Papillary	273	Reference		Reference		263	Reference		Reference		273	Reference		Reference	
Papillary	133	0.690 (0.487—0.976)	0.036	1.625 (0.663—3.980)	0.288	129	0.579 (0.372—0.900)	0.015	2.256 (0.709—7.184)	0.168	134	0.652 (0.459—0.926)	0.017	1.494 (0.636—3.509)	0.357
Lymphovascular invasion	280					272					281				
No	129	Reference		Reference		126	Reference		Reference		129	Reference		Reference	
Yes	151	2.247 (1.547—3.263)	< 0.001	1.999 (0.825—4.844)	0.125	146	2.975 (1.846—4.792)	< 0.001	2.162 (0.692—6.756)	0.185	152	2.313 (1.587—3.373)	< 0.001	1.090 (0.478—2.483)	0.838
Smoker	398					385					399				
No	109	Reference				105	Reference				109	Reference			
Yes	289	1.306 (0.923—1.849)	0.132			280	1.302 (0.857—1.977)	0.216			290	1.145 (0.818—1.603)	0.430		

Table 2 (continued)

	OS					DSS					PFI				
	Univariate analysis			Multivariate analysis		Univariate analysis			Multivariate analysis		Univariate analysis			Multivariate analysis	
Characteristics	Total(N)	HR(95% CI)	*P* value	HR(95% CI)	*P* value	Total(N)	HR(95% CI)	*P* value	HR(95% CI)	*P* value	Total(N)	HR(95% CI)	*P* value	HR(95% CI)	*P* value
Radiation therapy	385					374					386				
No	364	Reference				353	Reference				365	Reference			
Yes	21	0.967 (0.475—1.968)	0.926			21	1.018 (0.448—2.316)	0.966			21	1.256 (0.662—2.381)	0.485		
HSPG2	411					397					412				
Low	206	Reference		Reference		200	Reference		Reference		206	Reference		Reference	
High	205	1.654 (1.228—2.229)	< 0.001	2.204 (1.055—4.604)	0.036	197	1.727 (1.203—2.481)	0.003	2.693 (1.021—7.100)	0.045	206	1.445 (1.074—1.942)	0.015	2.392 (1.159—4.934)	0.018

Table 3 Multivariate COX analysis of HSPG2 and MESO prognosis

	OS					DSS					PFI				
	Univariate analysis			Multivariate analysis		Univariate analysis			Multivariate analysis		Univariate analysis			Multivariate analysis	
Characteristics	Total(N)	HR(95% CI)	P value	HR(95% CI)	*P* value	Total(N)	HR(95% CI)	*P* value	HR(95% CI)	*P* value	Total(N)	HR(95% CI)	*P* value	HR(95% CI)	*P* value
Pathologic T stage	84					65					82				
T1	14	Reference				11	Reference				13	Reference			
T2	25	0.977 (0.470—2.032)	0.950			21	0.679 (0.254—1.816)	0.440			25	0.921 (0.412—2.056)	0.841		
T3	32	1.056 (0.519—2.149)	0.880			22	0.953 (0.370—2.456)	0.921			32	0.860 (0.394—1.881)	0.706		
T4	13	0.775 (0.327—1.838)	0.563			11	0.821 (0.283—2.382)	0.716			12	0.611 (0.234—1.593)	0.314		
Pathologic N stage	82					62					80				
N0	44	Reference				36	Reference				42	Reference			
N1	10	0.919 (0.443—1.909)	0.822			5	0.380 (0.090—1.609)	0.189			10	0.604 (0.251—1.451)	0.259		
N2	25	0.805 (0.462—1.405)	0.446			19	0.627 (0.308—1.280)	0.200			25	0.642 (0.347—1.190)	0.159		
N3	3	1.753 (0.536—5.732)	0.353			2	1.535 (0.358—6.577)	0.563			3	1.768 (0.416—7.513)	0.440		
Pathologic M stage	60					54					59				
M0	57	Reference				51	Reference				57	Reference			
M1	3	1.856 (0.441—7.817)	0.399			3	2.327 (0.541—10.007)	0.257			2	1.094 (0.147—8.129)	0.930		
Pathologic stage	86					66					84				
Stage I	10	Reference				7	Reference				10	Reference			
Stage II	16	0.631 (0.265—1.507)	0.300			15	0.297 (0.094—0.937)	0.038			16	0.556 (0.221—1.401)	0.213		
Stage III	44	0.756 (0.359—1.592)	0.461			31	0.303 (0.107—0.860)	0.025			44	0.61 5 (0.280—1.349)	0.225		

Table 3 (continued)

	OS					DSS					PFI				
	Univariate analysis			Multivariate analysis		Univariate analysis			Multivariate analysis		Univariate analysis			Multivariate analysis	
Characteristics	Total(N)	HR(95% CI)	P value	HR(95% CI)	*P* value	Total(N)	HR(95% CI)	*P* value	HR(95% CI)	*P* value	Total(N)	HR(95% CI)	*P* value	HR(95% CI)	*P* value
Stage IV	16	0.705 (0.297—1.674)	0.428			13	0.390 (0.127—1.199)	0.100			14	0.448 (0.171—1.174)	0.102		
Gender	86					66					84				
Female	16	Reference				15	Reference				16	Reference		Reference	
Male	70	0.888 (0.494—1.595)	0.691			51	0.843 (0.424—1.676)	0.626			68	0.523 (0.285—0.961)	0.037	0.395 (0.207—0.752)	0.005
Age	86					66					84				
< =65	46	Reference				34	Reference				45	Reference			
>65	40	1.325 (0.826—2.125)	0.243			32	1.031 (0.563—1.887)	0.922			39	1.319 (0.787—2.210)	0.294		
Histological type	86					66					84				
Biphasic	23	Reference		Reference		18	Reference				22	Reference			
Diffuse malignant	5	0.575 (0.215—1.540)	0.271	0.638 (0.238—1.708)	0.371	5	0.766 (0.270—2.172)	0.616			4	0.834 (0.281—2.476)	0.743		
Epithelioid	57	0.497 (0.293—0.842)	0.009	0.586 (0.343—1.001)	0.051	42	0.506 (0.256—0.998)	0.049			57	0.496 (0.279—0.882)	0.017		
Sarcomatoid	1	3.418 (0.438—26.654)	0.241	2.718 (0.347—21.280)	0.341	1	0.000 (0.000—Inf)	0.997			1	0.000 (0.000—Inf)	0.997		
Residual tumor	35					34					34				
R0	17	Reference				16	Reference				17	Reference			
R1	3	0.634 (0.144—2.798)	0.548			3	1.501 (0.290—7.773)	0.628			3	0.796 (0.165—3.836)	0.777		
R2	15	1.223 (0.572—2.617)	0.604			15	2.786 (0.992—7.831)	0.052			14	2.510 (1.040—6.059)	0.041		
History asbestos exposure	69					51					68				
No	14	Reference				8	Reference				14	Reference			

Table 3 (continued)

	OS					DSS					PFI				
	Univariate analysis			Multivariate analysis		Univariate analysis			Multivariate analysis		Univariate analysis			Multivariate analysis	
Characteristics	Total(N)	HR(95% CI)	P value	HR(95% CI)	*P* value	Total(N)	HR(95% CI)	*P* value	HR(95% CI)	*P* value	Total(N)	HR(95% CI)	*P* value	HR(95% CI)	*P* value
Yes	55	0.988 (0.520—1.879)	0.972			43	1.391 (0.468—4.136)	0.553			54	1.590 (0.711—3.560)	0.259		
Laterality	86					66					84				
Bilateral	3	Reference				0	Reference				3	Reference			
Left	30	1.144 (0.344—3.799)	0.827			22	0.687 (0.357—1.321)	0.260			30	2.367 (0.316—17.720)	0.402		
Right	53	1.424 (0.441—4.606)	0.555			44					51	3.539 (0.485—25.812)	0.213		
Radiation therapy	85					65					83				
No	60	Reference				41	Reference				58	Reference			
Yes	25	0.682 (0.403—1.155)	0.155			24	0.761 (0.409—1.417)	0.389			25	0.805 (0.462—1.403)	0.444		
HSPG2	86					66					84				
Low	43	Reference		Reference		36	Reference		Reference		43	Reference		Reference	
High	43	2.447 (1.500—3.991)	< 0.001	2.219 (1.347—3.656)	0.002	30	3.056 (1.597—5.849)	< 0.001	3.056 (1.597—5.849)	< 0.001	41	1.835 (1.068—3.150)	0.028	2.264 (1.279—4.010)	0.005

Table 4 Multivariate COX analysis of OS of HSPG2 and KIRC

		Univariate analysis		Multivariate analysis	
Characteristics	**Total(N)**	**HR(95% CI)**	***P* value**	**HR(95% CI)**	***P* value**
Pathologic T stage	541				
T1	279	Reference		Reference	
T2	71	1.488 (0.893—2.478)	0.127	0.102 (0.008—1.338)	0.082
T3	180	3.321 (2.356—4.681)	< 0.001	0.468 (0.051—4.280)	0.501
T4	11	10.631 (5.374—21.03)	< 0.001	0.758 (0.057—10.123)	0.834
Pathologic N stage	258				
N0	242	Reference		Reference	
N1	16	3.422 (1.817—6.446)	< 0.001	0.368 (0.058—2.353)	0.291
Pathologic M stage	508				
M0	429	Reference		Reference	
M1	79	4.401 (3.226—6.002)	< 0.001	1.729 (0.144—20.81)	0.666
Serum calcium	367				
Low	204	Reference		Reference	
Normal	153	1.225 (0.865—1.735)	0.254	0.770 (0.437—1.357)	0.366
Elevated	10	4.846 (2.404—9.769)	< 0.001	0.621 (0.163—2.367)	0.485
Pathologic stage	538				
Stage I	273	Reference		Reference	
Stage II	59	1.183 (0.638—2.193)	0.594	7.364 (0.463—117.1)	0.157
Stage III	123	2.649 (1.767—3.971)	< 0.001	3.263 (0.330—32.24)	0.311
Stage IV	83	6.622 (4.535—9.670)	< 0.001	10.850 (0.378—311)	0.164
Gender	541				
Female	187	Reference			
Male	354	0.924 (0.679—1.257)	0.613		
Age	541				
< = 60	269	Reference		Reference	
> 60	272	1.791 (1.319—2.432)	< 0.001	1.735 (1.016—2.965)	0.044
Histologic grade	533				
G1	14	Reference		Reference	
G2	236	7,606,603.7579 (0.000—Inf)	0.993	11,012,291.1484 (0.000—Inf)	0.995
G3	207	14,061,844.0831 (0.000—Inf)	0.993	10,610,528.7864 (0.000—Inf)	0.995
G4	76	38,352,819.2469 (0.000—Inf)	0.993	16,380,378.5492 (0.000—Inf)	0.995
Hemoglobin	461				
Low	264	Reference		Reference	
Normal	192	0.430 (0.302—0.613)	< 0.001	0.693 (0.378—1.272)	0.236
Elevated	5	2.663 (0.844—8.400)	0.095	2.234 (0.260—19.21)	0.464
Laterality	540				
Left	253	Reference		Reference	
Right	287	0.707 (0.525—0.952)	0.022	1.287 (0.778—2.130)	0.326
HSPG2	541				
Low	270	Reference		Reference	
High	271	0.447 (0.325—0.614)	< 0.001	0.545 (0.311—0.954)	0.034

HSPG2 was negatively correlated with DNA repair, DNA damage and Apoptosis in UVM (Fig. 8b). HSPG2 expression was negatively correlated with DNA damage and invasion in OV (Fig. 8c).

Co-expressed genes and enrichment analysis of HSPG2

To further investigate the potential role of HSPG2 in tumorigenesis, we extracted 20 HSPG2-related genes from the GeneMANIA database for GO and KEGG

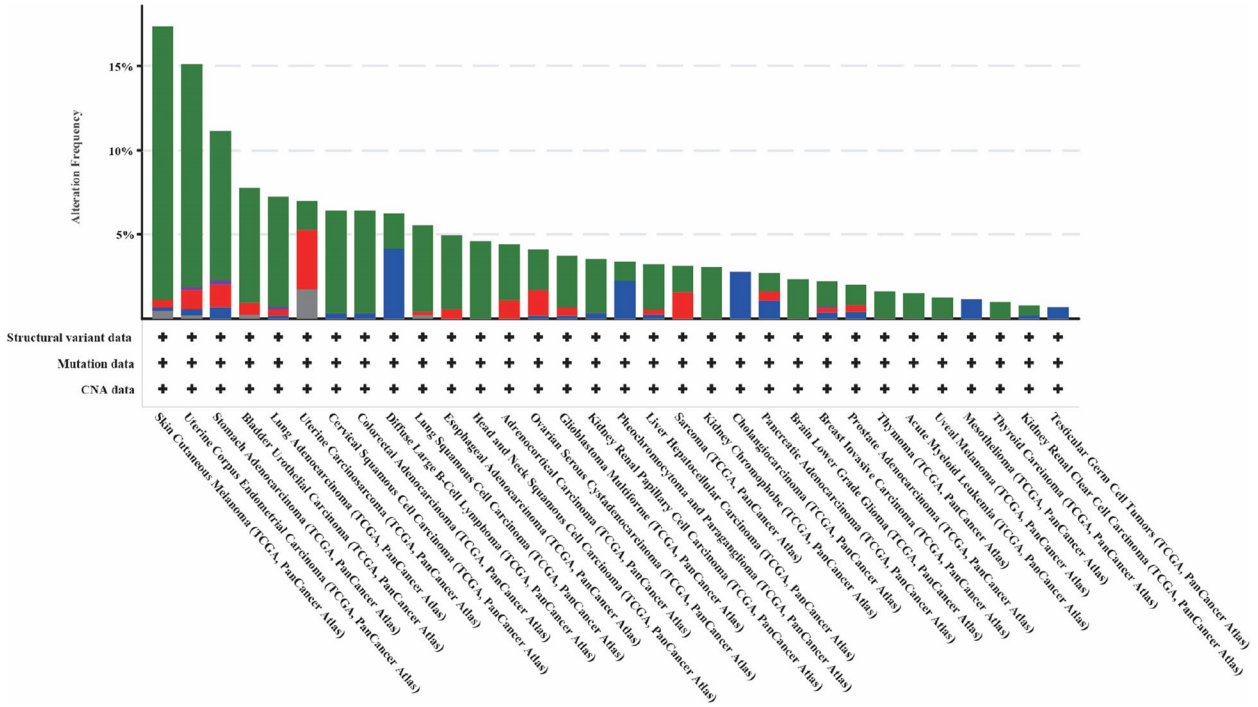

Fig. 4 Gene mutation analysis of HSPG2

enrichment analysis. Since only 20 co-expressed genes were obtained, we did not set additional screening criteria. The details are shown in Fig. 9.

Biological process (BP) enrichment analysis showed that HSPG2-related genes were mainly involved in negative regulation of glycoprotein metabolic process, extracellular matrix organization, extracellular structure organization and salivary gland development. In cellular component (CC) enrichment analysis, we found that HSPG2-related genes were enriched in collagen-containing extracellular matrix, basement membrane, tertiary granule lumen and chylomicron components. Molecular function enrichment (MF) analysis revealed that the role of HSPG2 in tumor pathogenesis was associated with extracellular matrix structural constituent, heparin binding, glycosaminoglycan binding and sulfur compound binding, glycosaminoglycan binding and sulfur compound, etc. In addition, KEGG pathway analysis showed that HSPG2-related genes were involved in some pathways, such as salivary secretion, PI3K-Akt signaling pathway and cholesterol metabolism.

Diagnostic efficacy of HSPG2 for BLCA and MESO and qPCR results and WB results

Since the mesothelioma control group is not included in TIMER and Xiantao Academic, in order to further analyze whether there are differences in the expression of HSPG2 in target diseases, especially between MESO and control group, GEO2R online analysis tool was used. The expression of HSPG2 in different disease states was analyzed by Benjamini & Hochberg method. The results showed that HSPG2 expression was different in MESO (adjusted *P*-value = 1.17e-4) and BLCA (adjusted *P*-value = 2.71e-5) compared with the control group. The rest details are shown in Fig. 10. The area under the curve (AUC) of HSPG2 for the diagnosis of BLCA and MESO were 0.650 (0.572–0.727) and 0.777 (0.683–0.872), respectively, and the results were shown in Figs. 10a and b. The qPCR results showed that the expression of HSPG2 was decreased in bladder cancer compared with human normal bladder cells ($P = 0.040$) (Fig. 10c), but HSPG2 expression was elevated in MESO ($P < 0.001$) (Fig. 10d). The results of WB also showed that HSPG2 protein was elevated in MESO (Fig. 10e).

Discussion

We revealed the molecular features of HSPG2 in 33 tumors from the perspectives of gene expression, prognosis, immune infiltration, DNA methylation, GO and KEGG enrichment analysis using various databases such as TCGA, GTEx, UALCAN, and cBioportal to elucidate its roles in the development and potential regulatory pathways of different tumors.

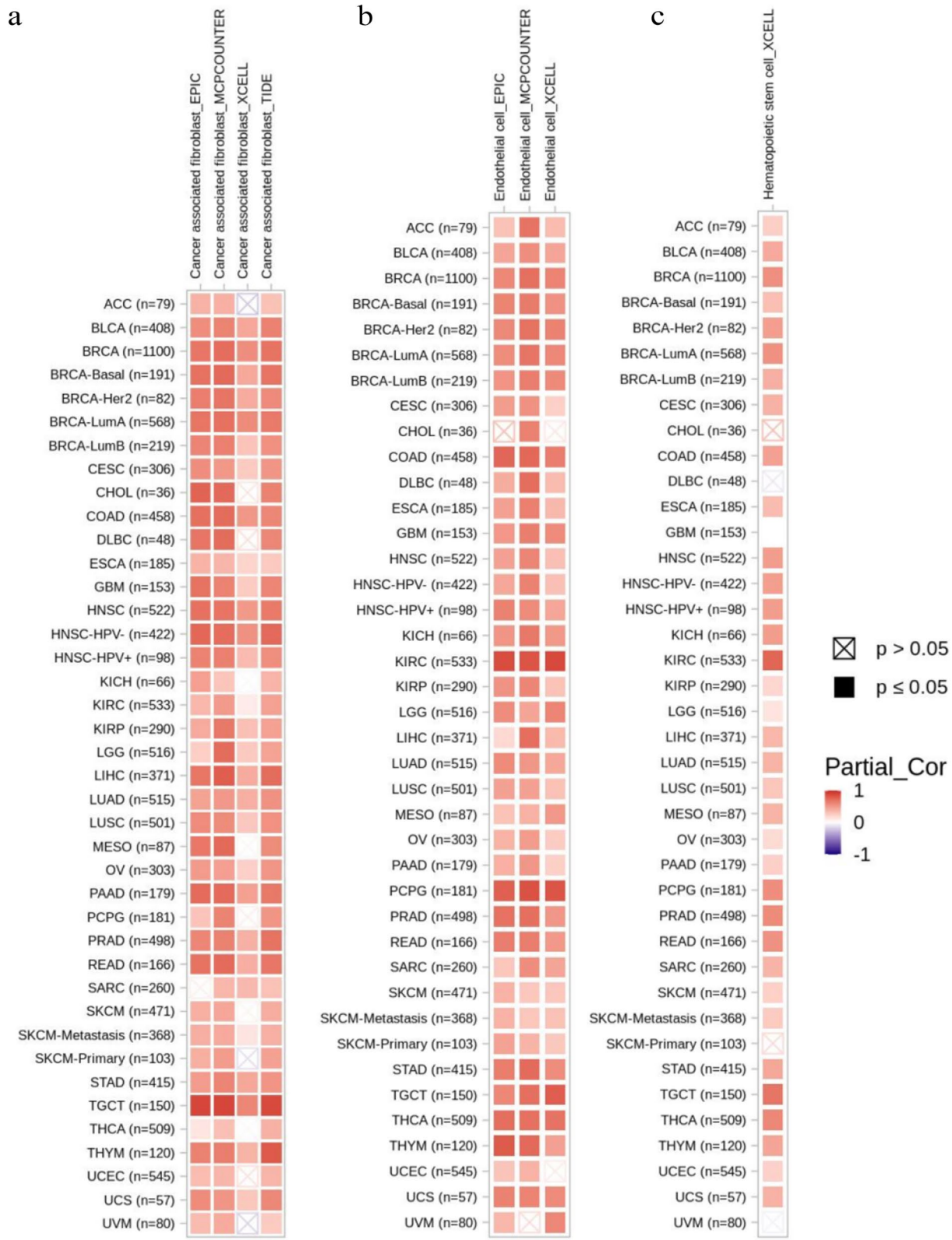

Fig. 5 Relationship between HSPG2 and Immunity. **a** Relationship between HSPG2 and cancer-associated fibroblasts; **b** relationship between HSPG2 and endothelial cells; **c** relationship between HSPG2 and hematopoietic stem cells

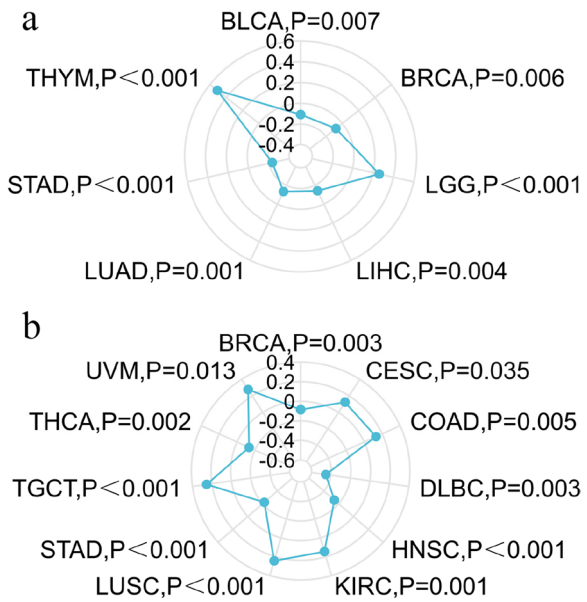

Fig. 6 Relationship between HSPG2 and TMB, MSI. **a** Relationship between HSPG2 and TMB; **b** relationship between HSPG2 and MSI

Our study showed that HSPG2 expression was up-regulated in 11 tumors and down-regulated in 17 tumors compared with controls, but the results of THCA were opposite in the TIMER database and TIMER plus GTEx database. The expression of HSPG2 was correlated with the T stage, N stage, and M stage of many cancers, as well as with patients' age and gender. In addition, both univariate and multivariate analyses showed that high expression of HSPG2 had shorter OS, DSS and PFI in BLCA and MESO, but low expression of HSPG2 had shorter OS in KIRC.

A growing number of studies have demonstrated that immune cell infiltration is a key factor in tumor progression and immunotherapy [37]. The results showed that HSPG2 expression was positively correlated with cancer-associated fibroblasts, endothelial cells, and hematopoietic stem cells in various kinds of tumors. Cancer-associated fibroblasts (CAFs) are a very heterogeneous cellular component of the tumor microenvironment characterized by a high degree of plasticity [38].

CAFs attract pro-tumoral myeloid cells (e.g., macrophages, granulocytes, dendritic cells (DCs), and myeloid-derived suppressor cells (MDSCs)), while myeloid cells infiltrate tumors and promote the tumorigenesis by facilitating tumor cell invasion and metastasis, supporting angiogenesis, and suppressing adaptive immune responses [39]. Another mechanism by which CAFs influence tumor growth is the secretion of pro-inflammatory cytokines that act directly on tumor cells and induce cell proliferation, anti-cell death and epithelial mesenchymal transition (EMT). Previous studies have shown that CAF respond to a variety of stimuli by secreting IL6, IL11 and LIF [40–42], and that these cytokines are key mediators of inflammation-driven tumorigenesis [43]. Tumor endothelial cell metabolism can be reprogrammed (e.g. glucose metabolism, amino acid metabolism, ketone body oxidation, etc.), and targeting endothelial metabolic pathways can affect growth and pathological vascular sprouting [44]. In addition, extracellular vesicles derived from tumor endothelial cells contribute to tumor microenvironment remodeling [45].

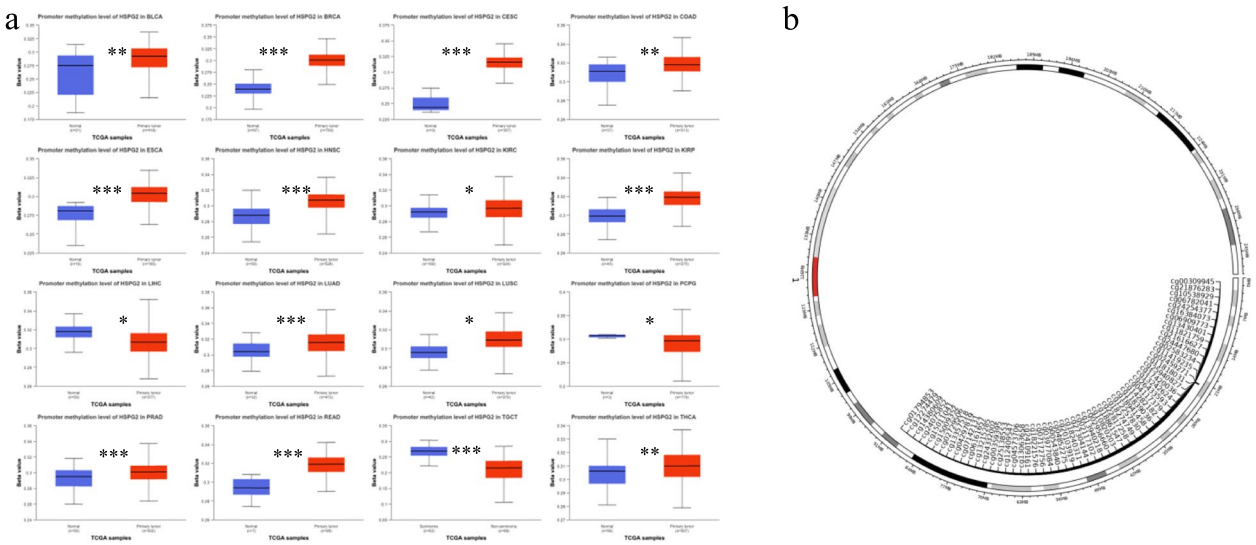

Fig. 7 Relationship between HSPG2 and promoter methylation and related methylation probes. **a** Relationship between HSPG2 and promoter methylation; **b** Methylation probes for HSPG2. * represents $P<0.05$, ** represents $P<0.01$, and *** represents $P<0.001$

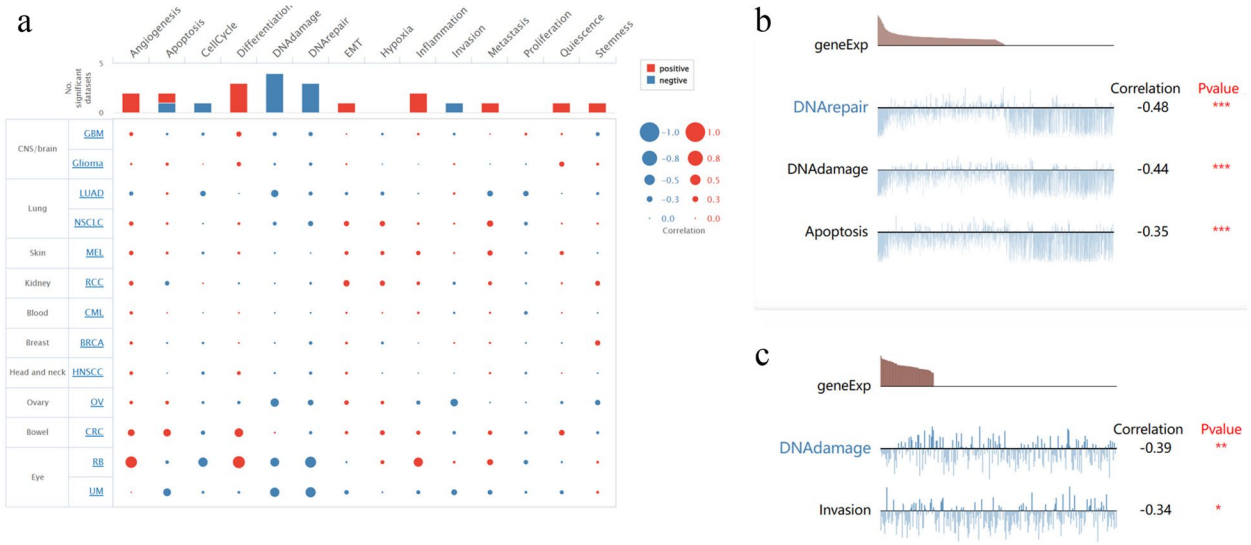

Fig. 8 Single-cell functional analysis of HSPG2. **a** Single-cell functional analysis of HSPG2; **b** relationship between HSPG2 and UVM; **c** relationship between HSPG2 and OV. * represents $P < 0.05$, ** represents $P < 0.01$, and *** represents $P < 0.001$

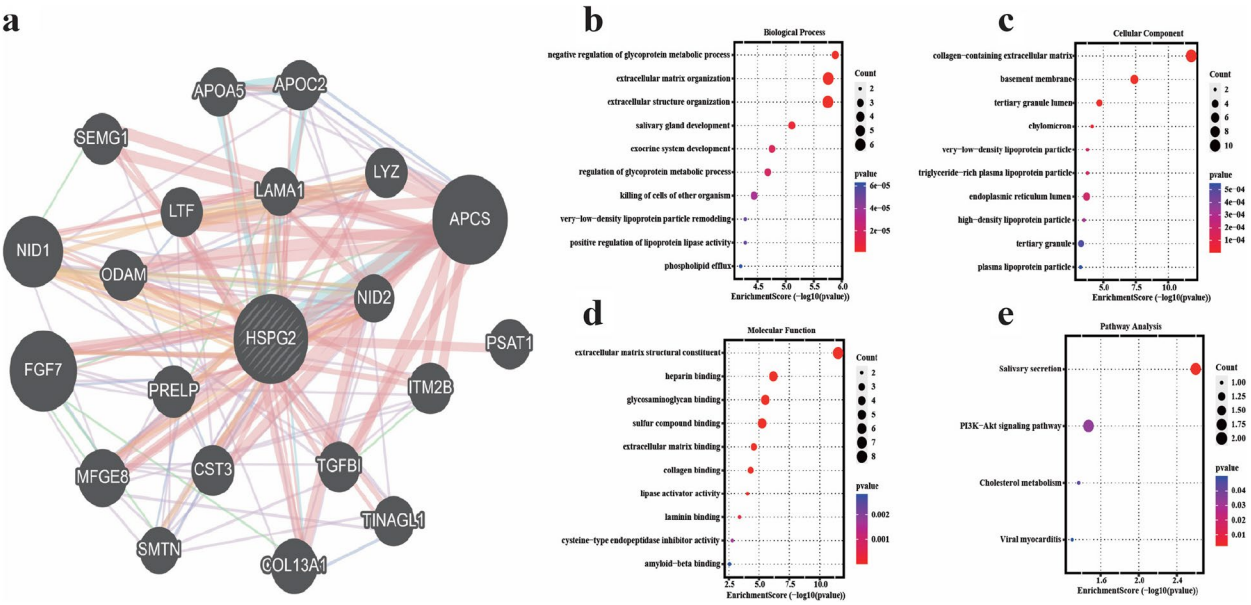

Fig. 9 Co-expressed genes and enrichment analysis of HSPG2. **a** Co-expressed genes of HSPG2; **b**-**d** GO enrichment analysis of co-expressed genes; **e** KEGG enrichment analysis of co-expressed genes

DNA methylation is one of the most common epigenetic modifications and plays an important role in gene expression, genome stability and tumorigenesis. It has been shown that aberrant DNA methylation may accelerate tumor development by regulating cell proliferation, thereby inducing apoptosis or senescence [46]. We observed that HSPG2 promoter methylation levels were increased in BLCA, BRCA, CESC, COAD, ESCA, HNSC, KIRC, KIRP, LUAD, LUSC, PRAD, READ, and THCA, and decreased in LIHC, PCPG, and TGCT, compared to normal tissues using the UALCAN tool.

In addition, we found that KEGG was enriched in the PI3K-AKT signaling pathway by analyzing the co-expressed genes of HSPG2. The PI3K/AKT signaling pathway is the most commonly activated pathway in cancer and can promote cancer cell growth, survival, and especially metabolism [47]. CAFs can also regulate cancer progression by altering the activity of the PI3K/AKT

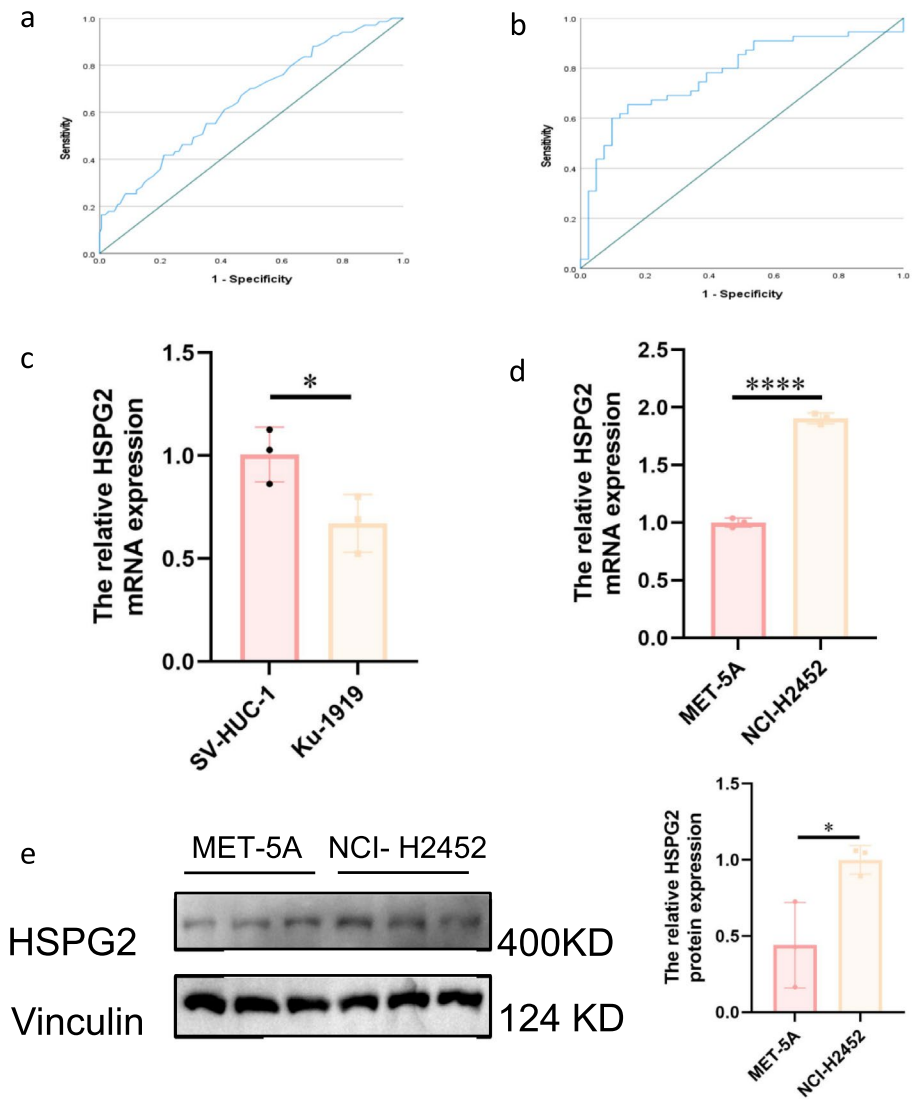

Fig. 10 The diagnostic efficacy of HSPG2 on BLCA and MESO and the expression of HSPG2 in four cell lines, and the results of WB. **a** The diagnostic efficacy of HSPG2 on BLCA; **b** The diagnostic efficacy of HSPG2 on MESO; **c** HSPG2 expression in bladder cancer (SV-HUC-1) and normal uroepithelium (Ku-1919); **d** HSPG2 expression in mesothelioma (NCI-H2452) and normal mesothelial cells (MET-5A); **e** The results of WB

pathway in cancer cells [48]. In addition to the previously described effects of endothelial cells on the tumor microenvironment, cancer cells can also promote endothelial cell tube formation and survival, at least in part, through the PI3K/AKT signaling pathway [49].

Although previous studies have shown that HSPG2 is associated with the prognosis of a variety of tumors, the present study finally demonstrated that HSPG2 may be an independent prognostic marker for BLCA and MESO. In addition, qPCR results showed that HSPG2 expression was decreased in bladder cancer compared with human normal bladder cells, and HSPG2 was increased in normal mesothelial cells compared with mesotheliomas, which was consistent with the results obtained by using the TIMER database and the Xiantao online analysis website, thus increasing further the reliability of the conclusions of the present study. More importantly, the prognostic value of HSPG2 in MESO was proposed for the first time. All these indicate the necessity of further research on the relevant mechanisms.

Although the role of HSPG2 in pan-cancer was analyzed in this study, some limitations should not be ignored. Firstly, all analyses were based on bioinformatics analysis, and the expression of HSPG2 was only confirmed by qPCR in some tumors. Secondly, after considering the molecular weight of HSPG2 (460 Kd),

our study did not investigate the molecular mechanism of HSPG2 in cancer. Further studies on the mechanism of HSPG2 expression in tumors are needed in the future. Thirdly, when analyzing the independent prognostic value of HSPG2, grouping according to the median amount of HSPG2 expression may result in a subset of otherwise differential results being negative.

Supplementary Information

The online version contains supplementary material available at https://doi.org/10.1186/s12920-025-02103-w.

Supplementary Material 1.

Acknowledgements
Not applicable.

Clinical trial number
Not applicable.

Authors' contributions
Conceptualization, Q.G. and C.F.; methodology, Q.G. and C.F.; software, C.F. and G.X.; investigation, C.F.; data curation, C.F. and G.X.; writing—original draft preparation, C.F. and G.X.; writing—review and editing, All authors; visualization, C.F.;supervision, Q.G.; project administration, Q.G.; funding acquisition, Q.G.. All authors have read and agreed to the published version of the manuscript.

Funding
This work was supported by Key Clinical Projects of Peking University Third Hospital [Grant No. BYSYRCYJ2023001].

Data availability
The datasets used and /or analysed during the current study available from the corresponding author on reasonable request.

Declarations

Ethics approval and consent to participate
Not applicable.

Consent for publication
Not Applicable.

Competing interests
The authors declare no competing interests.

Received: 8 October 2024 Accepted: 10 February 2025
Published online: 17 February 2025

References

1. Bray F, Laversanne M, Weiderpass E, Soerjomataram I. The ever-increasing importance of cancer as a leading cause of premature death worldwide. Cancer. 2021;127(16):3029–30.
2. You L, Lv Z, Li C, Ye W, Zhou Y, Jin J, Han Q. Worldwide cancer statistics of adolescents and young adults in 2019: a systematic analysis of the Global Burden of Disease Study 2019. ESMO Open. 2021;6(5):100255.
3. Siegel RL, Giaquinto AN, Jemal A. Cancer statistics, 2024. CA Cancer J Clin. 2024;74(1):12–49.
4. Teng Y, Xia C, Li H, Cao M, Yang F, Yan X, He S, Cao M, Zhang S, Li Q et al. Cancer statistics for young adults aged 20 to 49 years in China from 2000 to 2017: a population-based registry study. Sci China Life Sci. 2023;67(4):711–19.
5. Iozzo RV, Schaefer L. Proteoglycan form and function: A comprehensive nomenclature of proteoglycans. Matrix Biol. 2015;42:11–55.
6. Farach-Carson MC, Warren CR, Harrington DA, Carson DD. Border patrol: insights into the unique role of perlecan/heparan sulfate proteoglycan 2 at cell and tissue borders. Matrix Biol. 2014;34:64–79.
7. Lord MS, Tang F, Rnjak-Kovacina J, Smith JGW, Melrose J, Whitelock JM. The multifaceted roles of perlecan in fibrosis. Matrix Biol. 2018;68–69:150–66.
8. Warren CR, Grindel BJ, Francis L, Carson DD, Farach-Carson MC. Transcriptional activation by NFκB increases perlecan/HSPG2 expression in the desmoplastic prostate tumor microenvironment. J Cell Biochem. 2014;115(7):1322–33.
9. Grindel BJ, Martinez JR, Pennington CL, Muldoon M, Stave J, Chung LW, Farach-Carson MC. Matrilysin/matrix metalloproteinase-7(MMP7) cleavage of perlecan/HSPG2 creates a molecular switch to alter prostate cancer cell behavior. Matrix Biol. 2014;36:64–76.
10. Grindel BJ, Martinez JR, Tellman TV, Harrington DA, Zafar H, Nakhleh L, Chung LW, Farach-Carson MC. Matrilysin/MMP-7 Cleavage of Perlecan/HSPG2 Complexed with Semaphorin 3A Supports FAK-Mediated Stromal Invasion by Prostate Cancer Cells. Sci Rep. 2018;8(1):7262.
11. Zhou X, Liang S, Zhan Q, Yang L, Chi J, Wang L. HSPG2 overexpression independently predicts poor survival in patients with acute myeloid leukemia. Cell Death Dis. 2020;11(6):492.
12. Kalscheuer S, Khanna V, Kim H, Li S, Sachdev D, DeCarlo A, Yang D, Panyam J. Discovery of HSPG2 (Perlecan) as a Therapeutic Target in Triple Negative Breast Cancer. Sci Rep. 2019;9(1):12492.
13. Hu H, Li S, Cui X, Lv X, Jiao Y, Yu F, Yao H, Song E, Chen Y, Wang M, et al. The overexpression of hypomethylated miR-663 induces chemotherapy resistance in human breast cancer cells by targeting heparin sulfate proteoglycan 2 (HSPG2). J Biol Chem. 2013;288(16):10973–85.
14. Zhang W, Lin Z, Shi F, Wang Q, Kong Y, Ren Y, Lyu J, Sheng C, Li Y, Qin H et al. HSPG2 Mutation Association with Immune Checkpoint Inhibitor Outcome in Melanoma and Non-Small Cell Lung Cancer. Cancers. 2022;14(14):3495.
15. Ma XL, Shang F, Ni W, Zhu J, Luo B, Zhang YQ. Increased HSPG2 expression independently predicts poor survival in patients with oligoastrocytoma and oligodendroglioma. Eur Rev Med Pharmacol Sci. 2018;22(20):6853–63.
16. Kazanskaya GM, Tsidulko AY, Volkov AM, Kiselev RS, Suhovskih AV, Kobozev VV, Gaytan AS, Aidagulova SV, Krivoshapkin AL, Grigorieva EV. Heparan sulfate accumulation and perlecan/HSPG2 up-regulation in tumour tissue predict low relapse-free survival for patients with glioblastoma. Histochem Cell Biol. 2018;149(3):235–44.
17. Vennin C, Mélénec P, Rouet R, Nobis M, Cazet AS, Murphy KJ, Herrmann D, Reed DA, Lucas MC, Warren SC, et al. CAF hierarchy driven by pancreatic cancer cell p53-status creates a pro-metastatic and chemoresistant environment via perlecan. Nat Commun. 2019;10(1):3637.
18. Cohen IR, Murdoch AD, Naso MF, Marchetti D, Berd D, Iozzo RV. Abnormal expression of perlecan proteoglycan in metastatic melanomas. Can Res. 1994;54(22):5771–4.
19. Soloveva N, Novikova S, Farafonova T, Tikhonova O, Zgoda V. Proteomic Signature of Extracellular Vesicles Associated with Colorectal Cancer. Molecules. 2023;28(10):4227.
20. Nackaerts K, Verbeken E, Deneffe G, Vanderschueren B, Demedts M, David G. Heparan sulfate proteoglycan expression in human lung-cancer cells. Int J Cancer. 1997;74(3):335–45.
21. Rangel MP, de Sá VK, Prieto T, Martins JRM, Olivieri ER, Carraro D, Takagaki T, Capelozzi VL. Biomolecular analysis of matrix proteoglycans as biomarkers in non small cell lung cancer. Glycoconj J. 2018;35(2):233–42.
22. Wu Y, Liu Y, He A, Guan B, He S, Zhang C, Kang Z, Gong Y, Li X, Zhou L. Identification of the Six-RNA-Binding Protein Signature for Prognosis Prediction in Bladder Cancer. Front Genet. 2020;11:992.
23. Liu ZX, Zhang XL, Zhao Q, Chen Y, Sheng H, He CY, Sun YT, Lai MY, Wu MQ, Zuo ZX, et al. Whole-Exome Sequencing Among Chinese Patients With Hereditary Diffuse Gastric Cancer. JAMA Netw Open. 2022;5(12):e2245836.
24. Li T, Fan J, Wang B, Traugh N, Chen Q, Liu JS, Li B, Liu XS. TIMER: A Web Server for Comprehensive Analysis of Tumor-Infiltrating Immune Cells. Can Res. 2017;77(21):e108–10.

25. Uhlén M, Fagerberg L, Hallström BM, Lindskog C, Oksvold P, Mardinoglu A, Sivertsson Å, Kampf C, Sjöstedt E, Asplund A et al. Proteomics. Tissue-based map of the human proteome. Science. 2015;347(6220):1260419.
26. Liu X, Wu H, Liu Z. An Integrative Human Pan-Cancer Analysis of Cyclin-Dependent Kinase 1 (CDK1). Cancers. 2022;14(11):2658.
27. Cerami E, Gao J, Dogrusoz U, Gross BE, Sumer SO, Aksoy BA, Jacobsen A, Byrne CJ, Heuer ML, Larsson E, et al. The cBio cancer genomics portal: an open platform for exploring multidimensional cancer genomics data. Cancer Discov. 2012;2(5):401–4.
28. Li T, Fu J, Zeng Z, Cohen D, Li J, Chen Q, Li B, Liu XS. TIMER2.0 for analysis of tumor-infiltrating immune cells. Nucleic Acids Res. 2020;48(W1):W509-w514.
29. Steuer CE, Ramalingam SS. Tumor Mutation Burden: Leading Immunotherapy to the Era of Precision Medicine? J Clin Oncol. 2018;36(7):631–2.
30. Yang G, Zheng RY, Jin ZS. Correlations between microsatellite instability and the biological behaviour of tumours. J Cancer Res Clin Oncol. 2019;145(12):2891–9.
31. Ellegren H. Microsatellites: simple sequences with complex evolution. Nat Rev Genet. 2004;5(6):435–45.
32. Petrelli F, Ghidini M, Cabiddu M, Pezzica E, Corti D, Turati L, Costanzo A, Varricchio A, Ghidini A, Barni S, et al. Microsatellite Instability and Survival in Stage II Colorectal Cancer: A Systematic Review and Meta-analysis. Anticancer Res. 2019;39(12):6431–41.
33. Baylin SB, Jones PA. Epigenetic Determinants of Cancer. Cold Spring Harb Perspect Biol. 2016;8(9):a019505.
34. Li Y, Ge D, Lu C. The SMART App: an interactive web application for comprehensive DNA methylation analysis and visualization. Epigenetics Chromatin. 2019;12(1):71.
35. Yuan H, Yan M, Zhang G, Liu W, Deng C, Liao G, Xu L, Luo T, Yan H, Long Z, et al. CancerSEA: a cancer single-cell state atlas. Nucleic Acids Res. 2019;47(D1):D900-d908.
36. Franz M, Rodriguez H, Lopes C, Zuberi K, Montojo J, Bader GD, Morris Q. GeneMANIA update 2018. Nucleic Acids Res. 2018;46(W1):W60-w64.
37. Sadeghi Rad H, Monkman J, Warkiani ME, Ladwa R, O'Byrne K, Rezaei N, Kulasinghe A. Understanding the tumor microenvironment for effective immunotherapy. Med Res Rev. 2021;41(3):1474–98.
38. Kennel KB, Bozlar M, De Valk AF, Greten FR. Cancer-Associated Fibroblasts in Inflammation and Antitumor Immunity. Clin Cancer Res. 2023;29(6):1009–16.
39. Mantovani A, Marchesi F, Jaillon S, Garlanda C, Allavena P. Tumor-associated myeloid cells: diversity and therapeutic targeting. Cell Mol Immunol. 2021;18(3):566–78.
40. Biffi G, Oni TE, Spielman B, Hao Y, Elyada E, Park Y, Preall J, Tuveson DA. IL1-Induced JAK/STAT Signaling Is Antagonized by TGFβ to Shape CAF Heterogeneity in Pancreatic Ductal Adenocarcinoma. Cancer Discov. 2019;9(2):282–301.
41. Öhlund D, Handly-Santana A, Biffi G, Elyada E, Almeida AS, Ponz-Sarvise M, Corbo V, Oni TE, Hearn SA, Lee EJ, et al. Distinct populations of inflammatory fibroblasts and myofibroblasts in pancreatic cancer. J Exp Med. 2017;214(3):579–96.
42. Calon A, Espinet E, Palomo-Ponce S, Tauriello DV, Iglesias M, Céspedes MV, Sevillano M, Nadal C, Jung P, Zhang XH, et al. Dependency of colorectal cancer on a TGF-β-driven program in stromal cells for metastasis initiation. Cancer Cell. 2012;22(5):571–84.
43. Zhang C, Liu J, Wang J, Hu W, Feng Z. The emerging role of leukemia inhibitory factor in cancer and therapy. Pharmacol Ther. 2021;221:107754.
44. García-Caballero M, Sokol L, Cuypers A, Carmeliet P. Metabolic Reprogramming in Tumor Endothelial Cells. Int J Mol Sci. 2022;23(19):11052.
45. Gao J, Zhang X, Jiang L, Li Y, Zheng Q. Tumor endothelial cell-derived extracellular vesicles contribute to tumor microenvironment remodeling. Cell Commun Signal. 2022;20(1):97.
46. Pfeifer GP. Defining Driver DNA Methylation Changes in Human Cancer. Int J Mol Sci. 2018;19(4).
47. Courtney KD, Corcoran RB, Engelman JA. The PI3K pathway as drug target in human cancer. J Clin Oncol. 2010;28(6):1075–83.
48. Fang Z, Meng Q, Xu J, Wang W, Zhang B, Liu J, Liang C, Hua J, Zhao Y, Yu X, et al. Signaling pathways in cancer-associated fibroblasts: recent advances and future perspectives. Cancer Commun (Lond). 2023;43(1):3–41.
49. Cheng HW, Chen YF, Wong JM, Weng CW, Chen HY, Yu SL, Chen HW, Yuan A, Chen JJ. Cancer cells increase endothelial cell tube formation and survival by activating the PI3K/Akt signalling pathway. J Exp Clin Cancer Res. 2017;36(1):27.

Publisher's Note